ELSEVIER

Journal of Electroanalytical Chemistry 530 (2002) 16–22

Journal of Electroanalytical Chemistry

www.elsevier.com/locate/jelechem

Electrochemical investigation of lithium intercalation into graphite from molten lithium chloride

Qian Xu [1], Carsten Schwandt, George Z. Chen, Derek J. Fray *

Department of Materials Science and Metallurgy, University of Cambridge, Pembroke Street, Cambridge CB2 3QZ, UK

Received 9 May 2002; accepted 3 June 2002

Abstract

Lithium reduction at a graphite electrode in molten lithium chloride was studied at temperatures from 650 to 900 °C using cyclic voltammetry and chronoamperometry. It was found that, during cathodic polarization, lithium intercalation into graphite occurred before deposition of metallic lithium started. This process was confirmed to be rate-controlled by the diffusion of lithium in the graphite. When the cathodic polarization potential was more negative than that for metallic lithium deposition, exfoliation of graphite particles from the electrode surface was observed. This was caused by fast and excessive accumulation of lithium intercalated into the graphite, which produced mechanical stress too high for the graphite matrix to accommodate. The erosion process was abated once the graphite surface was covered by a continuous layer of liquid lithium. These results are of relevance to the mechanism of carbon nanotube and nanoparticle formation by electrochemical synthesis in molten lithium chloride.

Keywords: Lithium intercalation; Graphite; Molten salt electrochemistry

1. Introduction

The electrochemical synthesis, i.e. the electrolysis of molten alkali metal salts in the presence of a graphite cathode, is one of the promising ways to produce nano-sized carbon materials like tubes and particles in bulk quantities, since the method is comparatively simple and economic and also has the potential to be scaled up. The process has been described in several publications [1–4]. Thus far, it is known that the yield of nanotubes is dependent on the salt and the temperature applied as well as, in an interrelated manner, on the potential and the current density. A further process parameter is the reaction time, and it has been found that the yield of nanotubes starts to decrease after a certain electrolysis time [5].

In order to improve the process further, it is necessary to understand the mechanism of carbon nanotube formation in molten salts. Fray and coworkers [6,7] related the generation of carbon nanotubes to the intercalation of alkali metal into graphite, and proposed a mechanism for the electrolytic conversion of graphite into carbon nanotubes in molten salts. There is indeed some experimental evidence that alkali metal intercalation into graphite is an important step in the electrochemical synthesis [4,6], but a comprehensive and detailed knowledge of the overall process is still lacking.

This paper reports an electrochemical investigation into lithium reduction on a graphite electrode, using cyclic voltammetry and chronoamperometry, with the aim of elucidating the role of lithium intercalation into graphite in the formation process of nano-sized carbon materials in molten salts.

2. Theoretical considerations

The following electrochemical half-cell is considered.

molten LiCl | Li, graphite (1)

In what follows, it is assumed that the reduction of lithium ions of the molten lithium chloride at the graphite electrode may include both the intercalation

* Corresponding author. Tel./fax: +44-1223-334479

E-mail address: djf25@hermes.cam.ac.uk (D.J. Fray).

[1] On leave from: School of Materials Science and Metallurgy, Northeastern University, Shenyang 110004, PR China.

0022-0728/02/$ - see front matter
PII: S0022-0728(02)00998-1

of lithium into the graphite bulk and the electrodeposition of metallic lithium onto the graphite surface.

Case I. Intercalation of lithium into the graphite bulk. The intercalation process may be represented by the following equation.

$$Li^+ + e^- \Leftrightarrow (Li)_c \tag{2}$$

The term on the right-hand side of Eq. (2) denotes that the lithium intercalated into graphite is to be considered as the solute and the graphite as the solvent [8]. If the reduction process is rate-controlled by the diffusion of dissolved lithium in the graphite host lattice, with the concentration gradient located on the graphite side of the electrolyte | electrode interface, the corresponding current may be derived as follows.

The time-dependent diffusion in one dimension under semi-infinite linear transport conditions is described by Fick's second law.

$$\frac{\partial c_{Li}}{\partial t} = D_{Li}\frac{\partial^2 c_{Li}}{\partial x^2} \tag{3}$$

where t is the time, x is the space coordinate extending from the electrolyte | electrode interface into the graphite, c_{Li} is the local concentration of lithium in the graphite, and D_{Li} is the chemical diffusion coefficient of lithium in graphite. The appropriate initial and boundary conditions are as follows.

$$t = 0,\quad x \geq 0 \quad c_{Li} = 0 \tag{4}$$
$$t \geq 0,\quad x \to \infty \quad c_{Li} = 0 \tag{5}$$
$$t > 0,\quad x = 0 \quad c_{Li} = c_{Li}\ (x = 0) \tag{6}$$

Because of the assumption of a reversible electrode process, the lithium concentration in the graphite at the electrolyte | electrode interface is governed by the Nernst equation. It is suggested that, first, the concentration of lithium ions in pure molten lithium chloride is selected as the standard state for activity of lithium ions and, second, the saturation concentration of lithium in graphite is selected as the standard state for the activity of lithium in graphite. With this, the concentration of lithium at the surface of the graphite electrode can be expressed by the following equation.

$$c_{Li}(x = 0) = \frac{c^*_{Li}}{r_{Li}}\exp\left(-\frac{E - E^\circ}{RT}F\right) \tag{7}$$

where $c_{Li}\ (x = 0)$ is the lithium concentration in the graphite at the electrolyte | electrode interface, c^*_{Li} is the saturation concentration of lithium in graphite, r_{Li} is the Henrian activity coefficient of lithium in graphite, E is the potential applied, E° is the standard potential of the half-cell reaction expressed by Eq. (2), F is the Faraday constant, R is the universal gas constant, and T is the absolute temperature.

The time-dependent electric current $I(t)$ is then given by a modified Cottrell equation.

$$I(t) = -FSD_{Li}(\partial c_{Li}/\partial x) = FS(D_{Li}/\pi)^{1/2}\frac{c^*_{Li}}{r_{Li}}\exp\left(-\frac{E - E^\circ}{RT}F\right)\frac{1}{t^{1/2}} \tag{8}$$

where S is the geometric surface of the graphite electrode in contact with the salt melt.

If the current is reversed after a time period τ, the initial and boundary conditions are as follows.

$$t = \tau,\quad x \geq 0$$
$$c_{Li} = \frac{c^*_{Li}}{r_{Li}}\left(1 - \mathrm{erf}\frac{x}{2\sqrt{D_{Li}\tau}}\right)\exp\left(-\frac{E - E^\circ}{RT}F\right) \tag{9}$$
$$t > \tau,\quad x \to \infty \quad c_{Li} = 0 \tag{10}$$
$$t > \tau,\quad x = 0 \quad c_{Li} = 0 \tag{11}$$

Based on the same assumptions as above, the time-dependent electric current $I(t)$ is now given by the following equation.

$$I(t) = FSD_{Li}(\partial c_{Li}/\partial x) = -FS(D_{Li}/\pi)^{1/2}\frac{c^*_{Li}}{r_{Li}}\exp\left(-\frac{E - E^\circ}{RT}F\right) \times \left(\frac{1}{(t - \tau)^{1/2}} - \frac{1}{t^{1/2}}\right) \tag{12}$$

According to Eqs. (8) and (12), the relationships between $I(t)$ and $t^{-1/2}$ as well as $I(t)$ and $[(t-\tau)^{-1/2} - t^{-1/2}]$ should be linear, and the absolute values of the slopes should be equal for the same applied potential provided the process of lithium intercalation into graphite is reversible.

Case II. Deposition of lithium onto the graphite surface. If plain electrodeposition of lithium is the rate-controlling process, the current is determined by the electron transfer from the graphite onto the lithium ions in the salt melt. This type of kinetics is governed by the well-known Butler–Volmer equation and provides a time-independent electric current.

3. Experimental

Anhydrous lithium chloride was prepared by slow heating to 250 °C and holding at this temperature for more than 24 h in dry Ar. Experiments were performed using a three-terminal electrochemical cell. The working electrode (WE) was either a graphite rod of 6.5 mm diameter, shielded in an alumina tube and connected to a nickel lead, or a molybdenum wire of 0.5 mm diameter, likewise shielded in an alumina tube. A

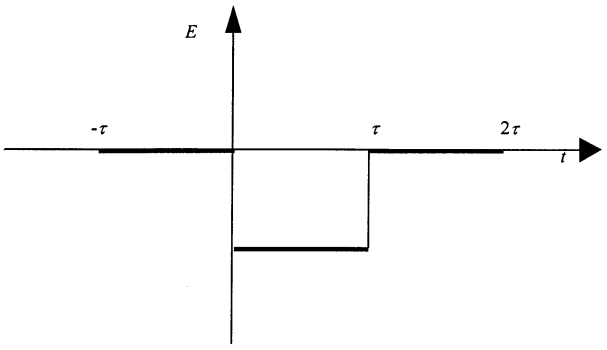

Fig. 1. Schematic representation of the perturbation potential as a function of time.

molybdenum wire was employed as the reference electrode (RE). A carbon crucible served as the container for the electrolyte and also as the counter electrode (CE). The electrochemical experiments were carried out in a sealable and water-cooled Inconel® reactor, positioned inside a programmable vertical tube furnace.

First, the WEs were characterized by means of cyclic voltammetry, applying scan rates of typically 100 mV s^{-1}. Second, the WEs were subjected to double potential step experiments. The perturbation potential as a function of time is sketched in Fig. 1. In order to simplify the mathematical description of the electrode process, a positive potential was initially applied, so it may be assumed that, at zero time, neither lithium dissolved in the graphite bulk nor lithium deposited on the graphite surface were present. The perturbation potential was then imposed for the time period A, ranging from 0 to τ, whereafter the potential was set back to the original value for the time period B, ranging from τ to 2τ. τ was typically 300 s. During the periods A and B, the current was recorded as a function of time. The electrochemical measurements were conducted at temperatures between 650 and 900 °C under dry Ar using the Solartron SI 1287 Electrochemical Interface or the Sycopel Scientific Powerstat. The stability of the RE potential was confirmed by measuring the potential difference between the molybdenum wire and a platinum wire in molten lithium chloride for more than 24 h. In the following, all potentials are expressed with respect to the molybdenum RE.

4. Results and discussion

Figs. 2 and 3 present cyclic voltammograms of the molybdenum wire and the graphite rod WEs in molten lithium chloride, respectively. Metallic lithium deposition on the molybdenum electrode occurs at a potential of −1.9 V at 650 °C. Reversing the potential scan then yields an anodic wave, which is typical for the stripping

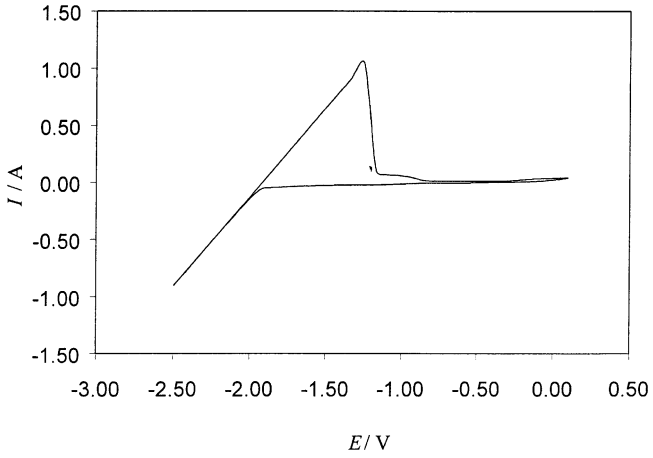

Fig. 2. Cyclic voltammogram for a molybdenum electrode in molten LiCl at a potential scan rate of $v = 100$ mV s^{-1} at 650 °C.

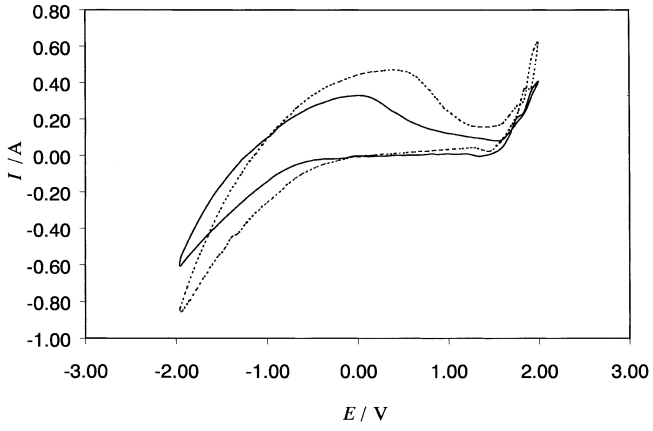

Fig. 3. Cyclic voltammograms for a graphite electrode in molten LiCl at a potential scan rate of $v = 100$ mV s^{-1} (solid line at 650 °C and dashed line at 900 °C).

of a previously adsorbed reaction product. The behaviour of lithium reduction on the graphite electrode is different from that on the molybdenum electrode. Discharge of lithium ions on the graphite electrode starts from potentials as high as −0.5 V at 650 °C. The reason for this shift of the discharge potential to considerably more positive values consists in the subsequent dissolution of the lithium reduced into the graphite bulk, a process that may take place at lithium activities far below unity. This is in fact the same phenomenon that causes the voltage degeneration in lithium batteries when graphite serves as the anode material [8,9]. It is also found that the potential of lithium reduction on the graphite electrode becomes more positive as the temperature increases. A possible reason is that the interaction between adjacent graphite layers decreases with rising temperature, thereby facilitating the intercalation process.

A typical chronoamperometric response curve of a graphite rod electrode in molten lithium chloride to a

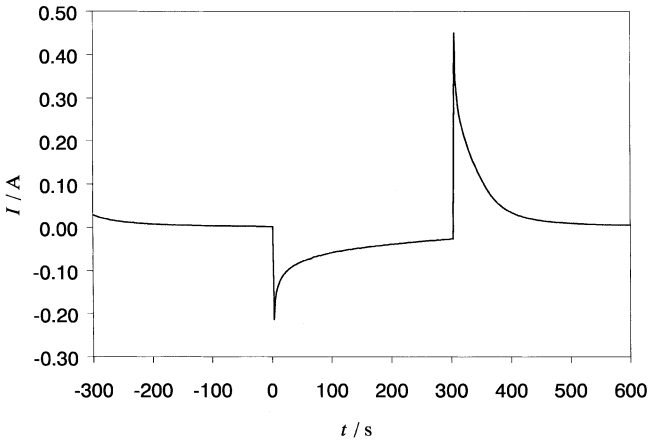

Fig. 4. A typical chronoamperometric response curve of a graphite electrode in molten LiCl to the double potential step of −1 V at 775 °C.

double potential step experiment of −1 V at 775 °C is shown in Fig. 4. It is suggested that the first peak, corresponding to period A, reflects the reduction of lithium from the salt melt followed by intercalation of the reduced lithium into the graphite bulk and that the second peak, corresponding to period B, represents the reverse reaction. However, according to Eq. (8), the $It^{1/2}$ values measured during period A should be independent of time, whereas it is found from Fig. 5 that these values change with time within a short interval after application of the potential, and this effect is more pronounced when larger potential steps are applied. Indeed, such an apparent discrepancy may be explained by means of an ohmic resistance in the circuit that influences the measurement despite the utilization of a RE [10]. This resistance originates from the fact that the WE and the RE are located on different equipotential lines, as a result of which, the electrolyte resistance is only partly eliminated in the three-terminal experiments performed. Because of this ohmic resistance in the circuit, the

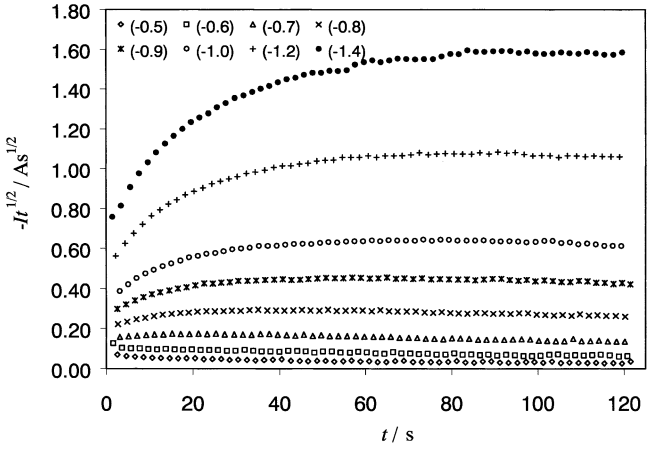

Fig. 5. Plot of $-It^{1/2}$ vs. t for a graphite electrode in molten LiCl at 775 °C (the data in parentheses are the potential steps (E/V)).

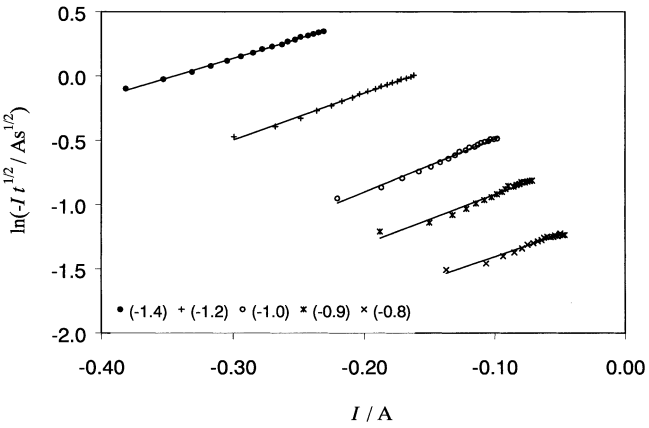

Fig. 6. Plot of $\ln[-It^{1/2}]$ vs. I for a graphite electrode in molten LiCl at 775 °C (the data in parentheses are the potential steps (E/V)).

potential E_c that is actually applied to the graphite electrode has to be expressed as

$$E_c = E - IR_\Omega \tag{13}$$

where R_Ω is the uncompensated ohmic resistance. On applying a potential step, the current changes quickly, and this gives rise to a fast change in the potential drop across the uncompensated ohmic resistance, too. For relatively large changes, as is the case immediately after application of the potential step and especially with higher potential steps, the ohmic voltage drop lowers the effective potential to a significant extent and causes the measured currents to deviate from those expected from Eq. (8). The relationships between $\ln(-It^{1/2})$ and I for time intervals ranging from 2 to 40 s after imposition of the potential are shown in Fig. 6. The slopes, which should depend on the ohmic resistance in the circuit, are linear and close to one another, and this is in agreement with the fact that the ohmic resistance in the circuit should be independent of the applied potential. When either the current or the change of the current with time

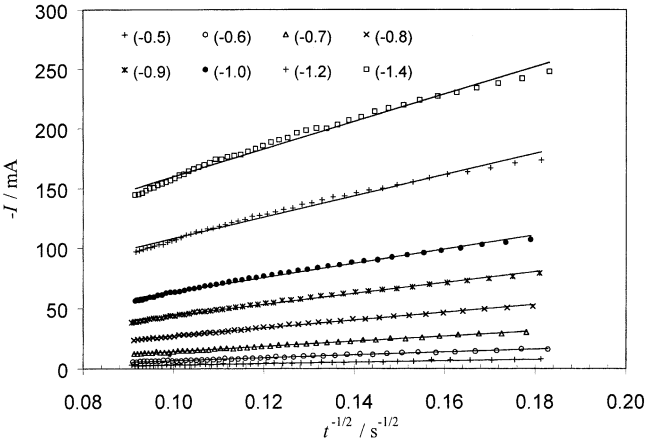

Fig. 7. Plot of $-I$ vs. $t^{-1/2}$ for a graphite electrode in molten LiCl during period A at 775 °C (the data in parentheses are the potential steps (E/V)).

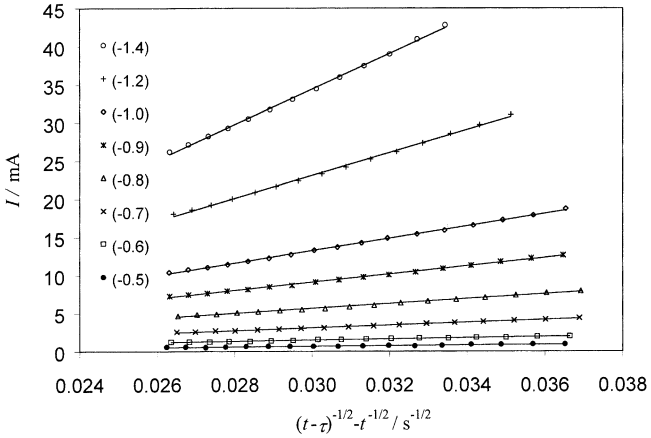

Fig. 8. Plot of I vs. $(t-\tau)^{-1/2}-t^{-1/2}$ at 775 °C for a graphite electrode in molten LiCl during period B (the data in parentheses are the potential steps (E/V)).

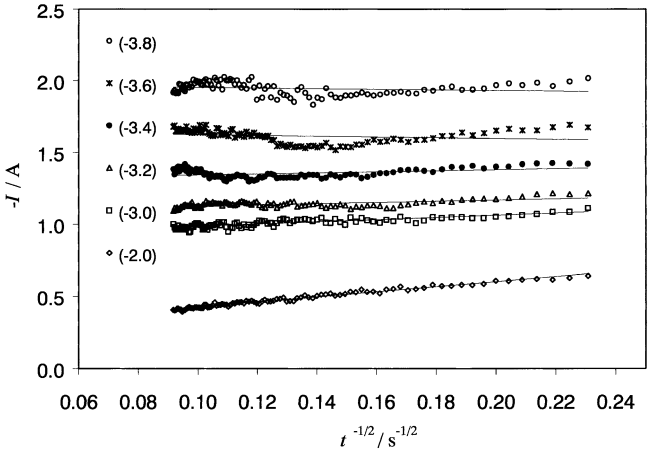

Fig. 9. Plot of $-I$ vs. $t^{-1/2}$ for a graphite electrode in molten LiCl during period A at 700 °C (the data in parentheses are the potential steps (E/V)).

becomes relatively small, the ohmic voltage drop is either negligible or may be considered as a constant, and then the relationship between current and time may indeed be described in terms of Eq. (8).

Fig. 7 shows the relationships between the current I and the reciprocal square root of time $t^{-1/2}$ measured between 60 and 120 s after application of the various potential steps during period A at 775 °C. Similar dependences were obtained for all other temperatures investigated between 650 and 900 °C. The slopes are linear in all cases, which, in accordance with Eq. (8), indicates that the reduction of lithium at potentials from −0.5 to −1.4 V is rate-controlled by the diffusion of intercalated lithium in the graphite matrix. Fig. 8 shows, the corresponding relationships between I and $[(t-\tau)^{-1/2}-t^{-1/2}]$ for period B at 775 °C and, in agreement with Eq. (12), the slopes are again found to be linear. The absolute values of the slopes obtained from the individual experiments during the periods A and B at different potential steps are summarised in Table 1. In

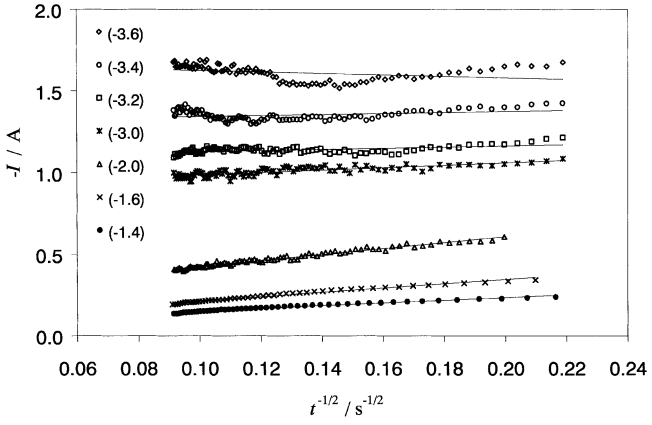

Fig. 10. Plot of $-I$ vs. $t^{-1/2}$ for a graphite electrode in molten LiCl during period A at 775 °C (the data in parentheses are the potential steps (E/V)).

both cases, the slopes increase with increasing potential, which is a consequence of the enhanced lithium con-

Table 1
The absolute values of the slopes for the plots of I vs. $t^{-1/2}$ (A) and I vs. $(t-\tau)^{-1/2}-t^{-1/2}$ (B) for different potential steps at temperatures from 650 to 900 °C

Temperature /°C	10 × (the absolute value of the slope)/A s$^{1/2}$							
	Potential step/V							
	−0.5	−0.6	−0.7	−0.8	−0.9	−1.0	−1.2	−1.4
650 (A)	0.23	0.44	0.88	1.6	2.4	3.3	5.4	9.2
(B)	0.13	0.21	0.71	0.90	2.2	4.3	9.4	16
700 (A)	0.31	0.65	1.3	2.1	3.2	4.3	6.8	9.8
(B)	0.31	0.27	0.70	1.7	3.4	5.7	12	20
775 (A)	0.59	1.2	2.1	3.3	4.5	5.9	8.9	12
(B)	0.40	0.78	1.8	3.2	5.4	8.2	15	23
850 (A)	1.2	2.0	2.9	3.9	5.3	6.8	9.1	12
(B)	0.92	1.8	3.2	5.4	8.2	12	22	45
900 (A)	1.5	2.2	3.2	4.5	5.7	6.9	9.6	14
(B)	1.1	2.1	3.6	5.8	9.1	12	19	45

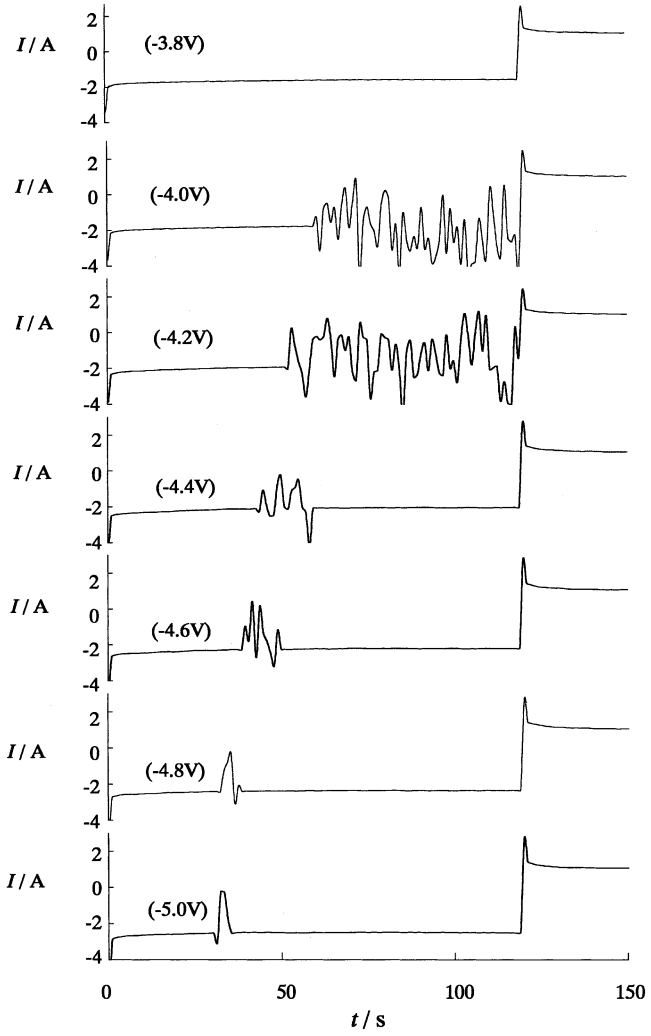

Fig. 11. Plot of I vs. t at 775 °C for a graphite electrode in molten LiCl at applied potential steps from −3.8 to −5.0 V.

centration gradient generated inside the graphite. Within experimental error, the slopes obtained for the periods A and B for corresponding experiments are fairly similar, so it can be concluded that lithium intercalation into graphite is an almost reversible process within the temperature range examined.

Figs. 9 and 10 show the relationships between I and $t^{-1/2}$ for the potential steps from −2.0 to −3.8 V at 700 °C and from −1.4 to −3.6 V at 775 °C, respectively. The absolute values of the slopes decrease with increasing potential steps, and at around −3.6 V the current becomes independent of time. This time-independent current is interpreted as the formation of a layer of elemental lithium on the surface of the graphite electrode, which is considered to be a simple electron transfer reaction, whilst the current associated with the intercalation process becomes negligible and no longer influences the current versus time behaviour. Accordingly, the potential range between −2.0 and −3.6 V is an intermediate range, in which both the intercalation of lithium into the graphite and the deposition of elemental lithium onto the graphite determine the current versus time plots.

When the potential applied during period A is more negative than −3.8 V, the current versus time plot exhibits abrupt fluctuations of the measured current. As becomes evident from Fig. 11, the higher the potential step, the sooner occurs the onset of these current spikes. It is thought that this current fluctuation is attributed to the repeated exfoliation of graphite particles from the electrode surface and the exposure of the fresh surface to the salt melt. Indeed, the occurrence of erosion on the graphite electrode during electrolyses carried out under these conditions is clearly visible after the experiments. Regarding the underlying reaction mechanism, it is straightforward to assume that, when a large amount of lithium intercalates into the graphite electrode in a short time, significant mechanical stress is generated inside the graphite matrix. When the diffusion of lithium is too slow to alleviate this stress, the attractive interaction between the graphite layers will eventually be exceeded, which then results in the observed exfoliation of graphite particles. As the lithium is present in high quantities and distributed homogeneously among the graphite layers, the exfoliated entities may be nano-sized at least in one dimension and may act as the precursors in the formation of nano-sized carbon materials like tubes and particles. Fig. 11 also illustrates that, for potentials more negative than −4.4 V, the exfoliation process may be abated after a certain amount of time, giving rise to constant currents again. The higher the potential step, the sooner this takes place. The finding is associated with the rapid build-up of a continuous film of liquid elemental lithium on the graphite electrode surface. As liquid lithium does not wet graphite very well, the mass transfer of lithium into the graphite and thus the intercalation process are slowed down, causing less erosion. It is likely that both the potential dependence and the time dependence observed in the lithium reduction at a graphite surface under high potentials have a direct impact on the yield of carbon nanotubes produced by means of this process.

5. Conclusions

From this study, it was found that lithium intercalates into a cathodically polarized graphite electrode from molten lithium chloride. When the potential applied to the graphite electrode is more positive than that for metallic lithium deposition, the cathodic current is controlled by the rate of lithium diffusion in the graphite. The process of lithium intercalation into graphite was found to be almost reversible within the investigated temperature range from 650 to 900 °C. When the potential applied is more negative than that

for metallic lithium deposition, exfoliation of graphite particles from the electrode surface occurs due to excessive lithium accumulation, causing destruction of the graphite matrix. The degree of exfoliation decreases when the graphite surface is covered completely by a layer of liquid lithium. The findings are of relevance to the preparation of nano-sized carbon materials with this method.

Acknowledgements

Qian Xu wishes to thank the China Scholar Council for financial support of her stay at the University of Cambridge.

References

[1] W.K. Hsu, J.P. Hare, M. Terrones, H.W. Kroto, D.R.M. Walton, P.J.F. Harris, Nature 377 (1995) 687.
[2] W.K. Hsu, M. Terrones, J.P. Hare, H. Terrones, H.W. Kroto, D.R.M. Walton, Chem. Phys. Lett. 262 (1996) 161.
[3] G.Z. Chen, X. Fan, A. Luget, M.S.P. Shaffer, D.J. Fray, J. Electroanal. Chem. 446 (1998) 1.
[4] G. Kaptay, I. Sytchev, J. Miklósi, P. Nagy, P. Póczik, K. Papp, E. Kálmán, in: R.W. Berg, K.A. Hjuler (Eds.), Progress in Molten Salt Chemistry 1, Elsevier, Amsterdam, 2000, p. 257.
[5] I. Kinloch, Thesis, University of Cambridge, 2001.
[6] G.Z. Chen, I. Kinloch, M.S.P. Shaffer, D.J. Fray, A.H. Windle, High Temp. Mater. Process. 2 (1998) 459.
[7] D.J. Fray, High Temp. Mater. Process. 3 (1999) 67.
[8] M. Jean, C. Desnoyer, A. Tranchant, R. Messina, J. Electrochem. Soc. 142 (1995) 2122.
[9] D. Aurbach, Y. Ein-Eli, B. Markovsky, A. Zaban, S. Luski, Y. Carmeli, H. Yamin, J. Electrochem. Soc. 142 (1995) 2882.
[10] C. John Wen, B.A. Boukamp, R.A. Huggins, W. Weppner, J. Electrochem. Soc. 126 (1979) 2258.